Journal of the Meteorological Society of Japan, Vol. 92, No. 4, pp. 385−405, 2014
DOI:10.2151/jmsj.2014-407

Mitigation of Sri Lanka Island Effects in Colombo Sounding Data and Its Impact on DYNAMO Analyses

Paul E. CIESIELSKI, Richard H. JOHNSON

Department of Atmospheric Science, Colorado State University, Colorado, USA

Kunio YONEYAMA

Japan Agency for Marine-Earth Science and Technology, Yokosuka, Japan

and

Richard K. TAFT

Department of Atmospheric Science, Colorado State University, Colorado, USA

(Manuscript received 6 February 2014, in final form 28 March 2014)

Abstract

During the Dynamics of the MJO (DYNAMO) field campaign in 2011, upper-air soundings were launched in Colombo, Sri Lanka, as part of the enhanced northern sounding array (NSA) of the experiment. The Colombo soundings were affected at low levels by the diurnal heating of this large island and by flow blocking caused by elevated terrain to the east of the Colombo site. Because of the large spacing between sounding sites, these small-scale island effects are aliased onto the larger scale impacting analyses and atmospheric budgets over the DYNAMO NSA. To mitigate these local island effects on the large-scale budgets, a procedure was designed that used low-level ECMWF-analyzed fields in Sri Lanka's vicinity to estimate open-ocean conditions at Colombo's location as if the island were not present. These "unperturbed" ECMWF fields at low-levels were then merged with the observed Colombo soundings. Results indicate a beneficial impact of using these adjusted fields on several aspects of the budget analyses.

Keywords DYNAMO; upper-air soundings; island-effects; atmospheric budgets

1. Introduction

A primary component of the observing system in the Dynamics of MJO (DYNAMO)/Cooperative Indian Ocean experiment on intraseasonal variability in the Year 2011 (CINDY2011)/ARM MJO investigation experiment (AMIE) field campaign (hereafter referred to as DYNAMO) was an atmospheric sounding network comprising two sounding quadrilaterals, one north and the other south of the equator, over the central Indian Ocean (Yoneyama et al. 2013). The northern sounding array (NSA) is shown in Fig. 1. As observed in this figure, there is a substantial north–south mountain range located ~100 km to the east of the sounding site in Colombo, Sri Lanka. This topographic feature with a high point[1] of ~1700 m had a significant impact on the low-level flow over

Corresponding author: Paul E. Ciesielski, Department of Atmospheric Science, Colorado State University, Fort Collins, Colorado 80523, USA
E-mail: paulc@atmos.colostate.edu

[1]1700 m is the high point when using 1/6° resolution topographic data. Highest point in Sri Lanka is actually Mt. Pedro at 2524 m.

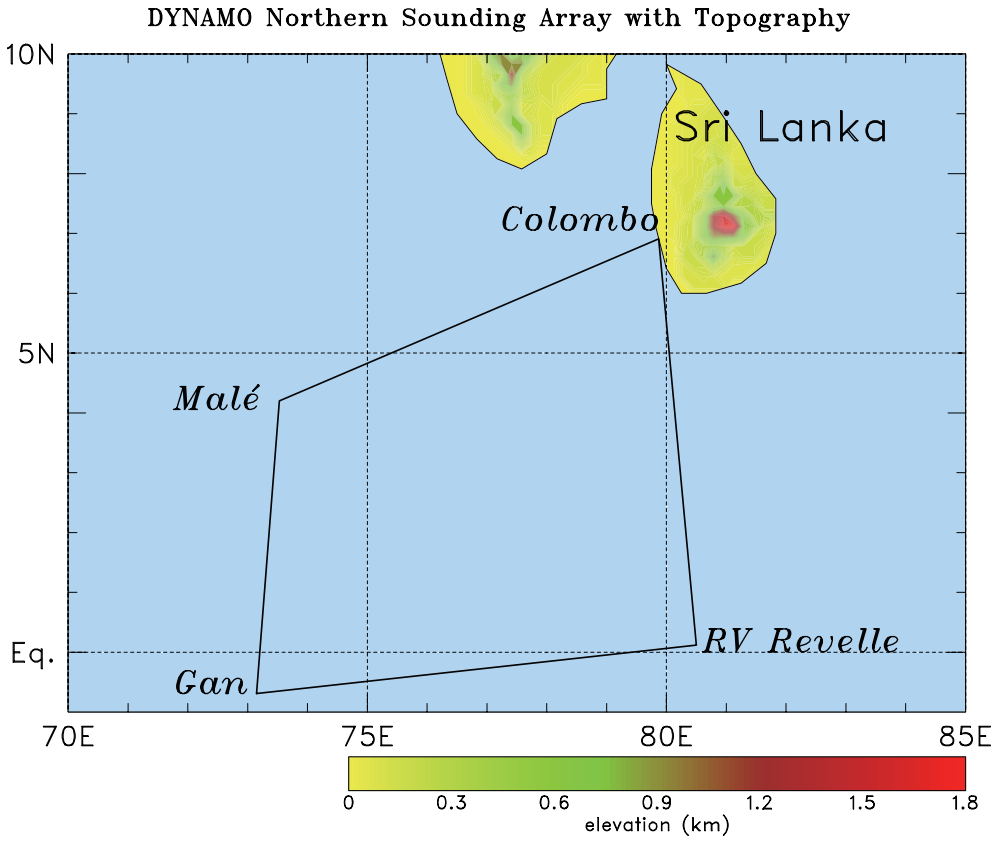

Fig. 1. DYNAMO Northern Sounding Array (NSA) showing the topographic features over Sri Lanka and India. Elevation (km) scale bar is shown at the bottom.

Sri Lanka, particularly at Colombo, where 258 soundings were taken four times daily primarily during the DYNAMO special observing period (SOP) from 1 October to 30 November 2011. In addition, the large size (~66,000 km^2) and elevated terrain of Sri Lanka result in a robust diurnal heating over the island, which significantly impacts low-level fields in the island's proximity (Zubair 2002).

During the SOP, two MJO events propagated through this region (Johnson and Ciesielski 2013) causing systematic changes in the flow regime on the MJO time scale (30–40 days). For example, Figs. 2 and 3 show the 925 hPa flow and moisture from the ECMWF operational analysis in low-level westerly and easterly wind regimes, respectively, and the associated flow blocking around Sri Lanka. In both regimes, topographic blocking alters the low-level wind flow and moisture fields at Colombo from the state that would exist if no barriers were present.

Special considerations for topographic effects were made in constructing budget analyses for the South China Sea monsoon experiment (SCSMEX) field campaign (Johnson and Ciesielski 2002) conducted in May and June 1998. In that study, the low-level flow at the Laoag, Philippines, sounding site was affected by a 2–3 km mountain range directly to its east. Specifically, prior to the onset of monsoon in that region, localized blocking of the low-level easterly flow resulted in weak flows at Laoag, which were aliased onto larger scales by the objective analysis scheme because of the sparse sounding network spacing. This aliased flow led to excessive low-level divergence and subsidence over the sounding array and unrealistically negative precipitation rates, as deduced from the moisture budget. To lessen the impact of the blocking effects at this site, the Laoag sounding winds below 700 hPa were replaced by reanalysis winds from a nearby model gridpoint, which were unaffected by the barrier blocking. As in SCSMEX, the large spacing between DYNAMO

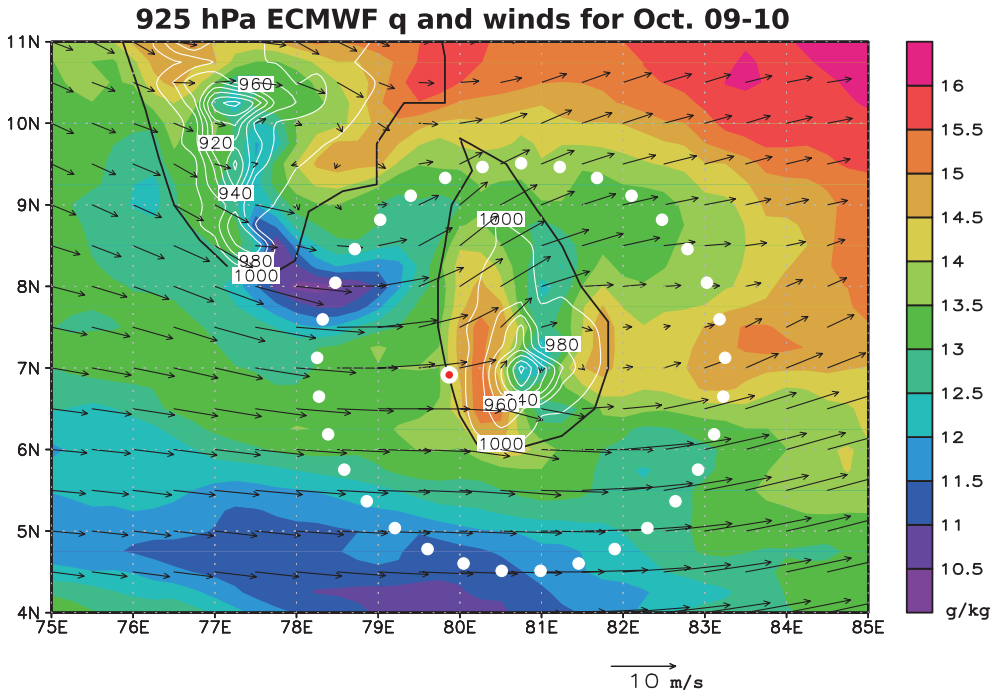

Fig. 2. ECMWF operational analysis of water vapor mixing ratio q and winds at 925 hPa averaged over a two day period (09–10 October 2011) showing flow blocking around topographic features. Wind scale (10 m s^{-1}) is shown below plot and scale for q to right of plot. ECMWF surface pressure analysis (white labeled contours) gives an indication of topographic features in the model. Ring of white circles shows 2.5° sampling radius used in the adjustment procedure. Red filled white circle shows location of Colombo sounding site.

sounding sites (Fig. 1) causes the local island heating and blocking effects at Colombo to be aliased onto larger scales, adversely impacting analyses over the NSA, and in turn, the computation of atmospheric budgets.

An alternative to using the "island perturbed" Colombo soundings in the budget analysis is to simply disregard this data source. In this scenario, the analyses would be based on a triangular sounding array similar to that used in the *Mirai* Indian Ocean cruise for the study of the MJO onset (MISMO) experiment (Yoneyama et al. 2008). Analysis based on sounding data from the MISMO network exhibited large discrepancies between budget-derived rainfall and independent estimates during the convectively active MJO phase (Katsumata et al. 2011). Utilizing model-simulated MJO circulations, their study found that periods with poor budget-derived rainfall resulted from the inability of the MISMO triangular network to properly capture the divergence associated with the Rossby and inertia–gravity wave components of the circulation. Furthermore, they demonstrated that a rectangular array was superior in capturing the divergence signal associated with these wave disturbances. Ultimately, this recommendation encouraged DYNAMO organizers to design its sounding network with a rectangular configuration. This experience motivates this study to determine a reasonable approach for using the Colombo soundings in budget analyses.

An important goal of DYNAMO, aimed at a better understanding of MJO initiation and convection, is to develop accurate forcing datasets, which are representative of large-scale oceanic conditions over the Indian Ocean, for use in cloud-resolving and single-column models. Since these datasets are used to force models, our practice has been to keep these products as independent as possible from model analyses, which are influenced by various parameterization schemes, a source of model infidelity. In this study, we relax this requirement in order to develop an adjustment procedure that utilizes ECMWF operational analyses (OA) in a limited manner to mitigate the local island effects on the Colombo sound-

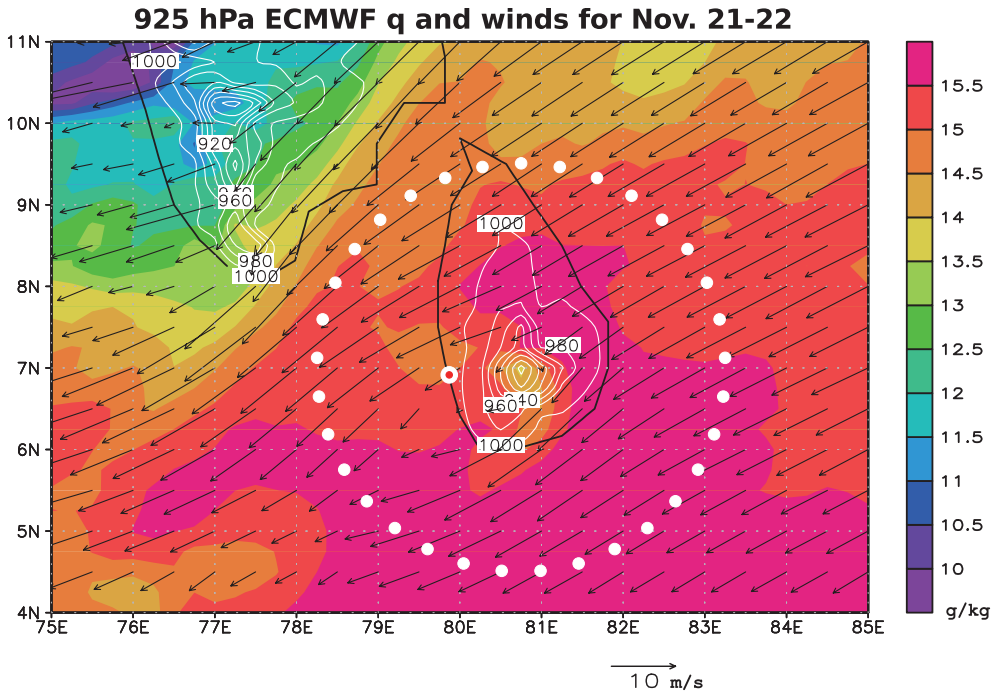

Fig. 3. As in Fig. 2, except for two-day period (21–22 November 2011).

ings. The outline of this paper is as follows. Section 2 describes the data sources used in this study and the sounding adjustment procedure. The temporal and vertical structure of the adjustment and its impact on various fields and analyses are examined in Sections 3 and 4, respectively. A summary is provided in Section 5.

2. Data sources and adjustment procedure

a. Data sources

With a stated goal of adjusting the Colombo sounding fields to mitigate the local island effects, we use the ECMWF OA, which is available every 6 h at 0.25° horizontal resolution with 18 vertical levels from surface to 50 hPa. Sounding data used in this study were quality-controlled and corrected, as described in Ciesielski et al. (2014). The corrections at Colombo were limited to the moisture variable, and moistened soundings slightly below 800 hPa and dried them in a deep layer above this level. Uncorrected soundings were assimilated in real time into the ECMWF OA, resulting in mean biases and rms differences between humidity-corrected soundings and model fields at this site that are reasonably small (Fig. 4). For example, wind biases were less than 1 m s^{-1} at any given level in the troposphere. The model's cool and dry biases observed here at low levels were observed at all NSA sites (not shown) and are consistent with the findings of Nagarajan and Aiyyer (2004) who examined ECMWF model biases over the Indian Ocean using prior field campaign sounding datasets. In their study, they attribute the model's low-level cool bias to excessive longwave clear-sky cooling associated with the water vapor continuum in the analysis. While these small biases suggest that this OA product captured the blocking effects at Colombo, the large-scale flow surrounding Sri Lanka (see Figs. 2, 3) is also well represented in the ECMWF analysis by its assimilation of many data sources in addition to upper-air soundings (e.g., cloud-drift and scatterometer winds, COSMIC data, and satellite irradiances). The idea here is to sample the large-scale ECMWF OA fields far enough away from Sri Lanka to be only marginally perturbed by the island, and then to use this information to estimate what the unperturbed fields would be at Colombo's location.

Other data sources used in this study include the tropical rainfall measuring mission (TRMM) 3B42v7 rainfall analyses (Huffman et al. 2007), which is available every 3 h at 0.25° horizontal resolution. To compute budget-derived rainfall as a residual from the moisture budget (Yanai et al. 1973), surface

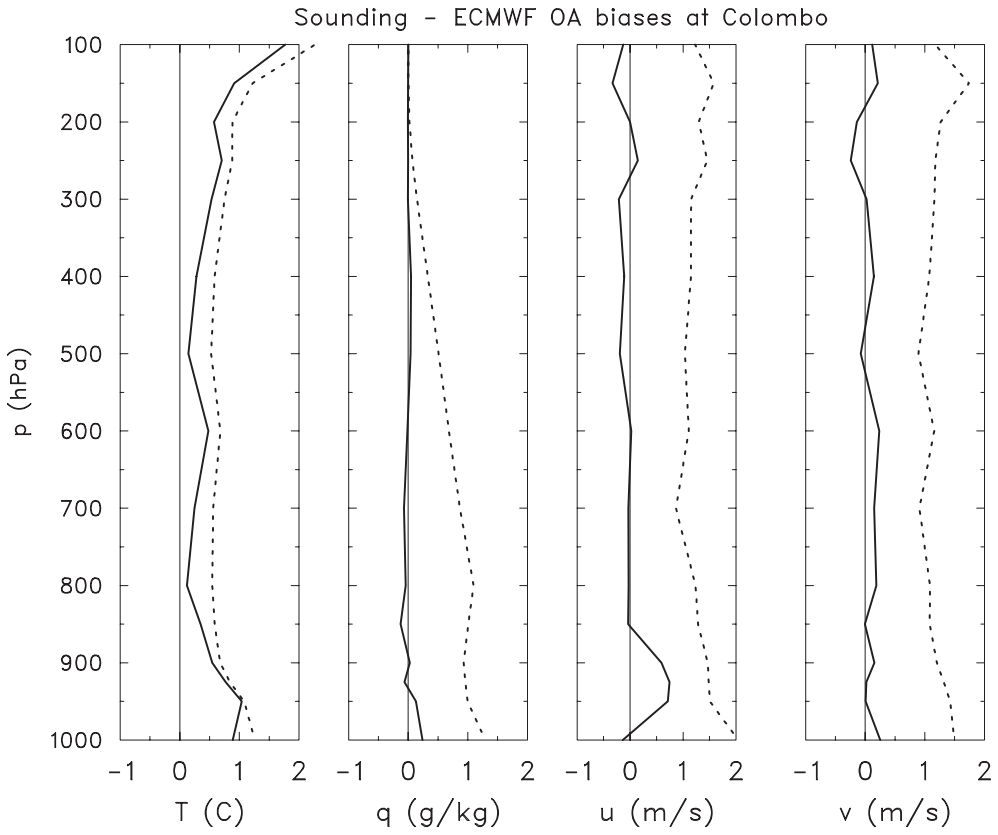

Fig. 4. Mean biases (solid) and rms differences (dashed) between soundings and ECMWF OA at Colombo for: (a) temperature, (b) water vapor mixing ratio, (c) zonal wind, and (d) meridional wind.

latent heat fluxes were obtained from the Woods Hole Oceanographic Institute (WHOI) objectively analyzed air-sea flux product (Yu and Weller 2007).

b. Vertical extent of the island's impact

The vertical extent of the island's impact on the Colombo sounding fields can be surmised from Fig. 5, which shows the vertical structure of the diurnal cycle anomaly of the basic sounding fields. The atmospheric response to the island's diurnal cycle of heating/cooling, observed clearly below 900 hPa, results in a robust daytime sea breeze and nighttime land breeze at Colombo. The return flow from these circulation cells extends to approximately 800 hPa. These land/sea breezes contribute to a daytime boundary layer moistening and nighttime drying. By comparison, the diurnal cycle of its nearest neighboring sounding site (Malé, Maldives at 4.2°N, 73.5°E) shows little amplitude difference in the diurnal cycle anomaly between the boundary layer and the free troposphere (Fig. 6). The Malé site, which also launched 4 day^{-1} soundings during this period, is more representative of the open ocean, being located on a small island with no topographic features over 2 m.

Another means to assess the island's impact on Colombo winds and the vertical extent of the flow blocking is by comparing the vertical-lag autocorrelation of sounding winds at Colombo with those at Malé. The vertical-lag autocorrelation of winds for these two sites is shown in Figs. 7 and 8 for base points at five different pressure levels (1000, 900, 800, 700 and 600 hPa). The island's impact at Colombo is seen in the e-folding distance for correlation decay, which is much smaller at Colombo than at Malé. For example, the e-folding distance for the zonal-wind correlation decay with a base point at 1000 hPa is ~100 hPa at Colombo (Fig. 7, upper right) and over 500 hPa at Malé (Fig. 8, upper right). Relative to Malé, correlations at Colombo decay more rapidly with height below 800 hPa with the rate of decorrelation increasing below 900 hPa. Consistent with the diurnal cycle anomalies induced by the

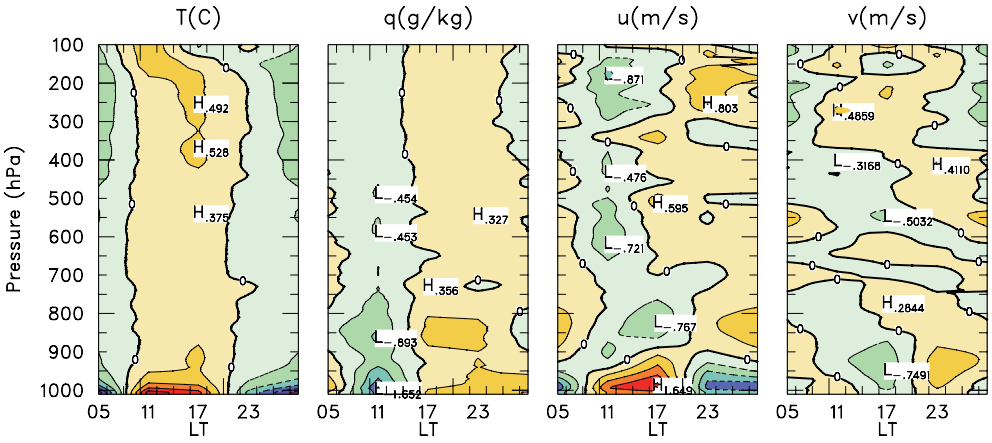

Fig. 5. Diurnal cycle anomaly (mean at each 5-hPa level has been subtracted) of original fields at Colombo as a function of pressure. Contour increment is 0.5 for all fields. Positive (negative) anomalies are depicted with warm (cool) shading.

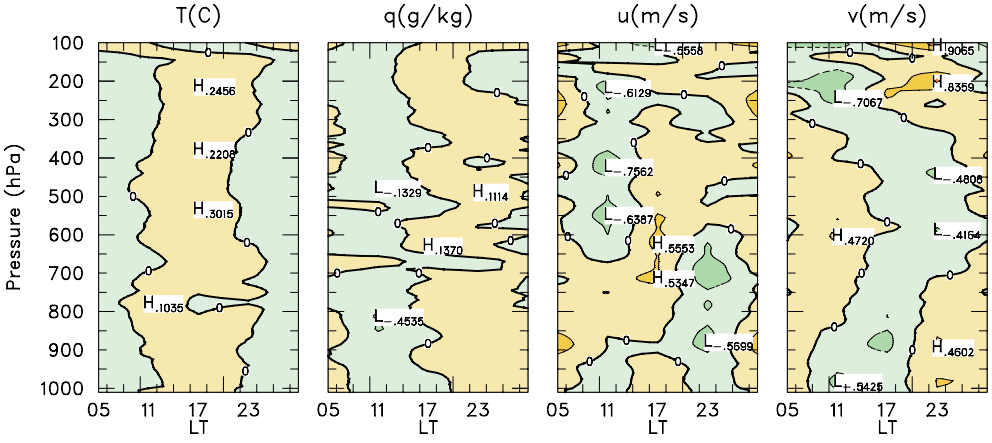

Fig. 6. As is Fig. 5, except for Malé.

island (Fig. 5), these correlation analyses suggest that the island's impact on Colombo soundings is confined primarily to ~800 hPa (or 2 km) and below. This height also seems reasonable for flow blocking impacts, considering the island's topography shown in Fig. 1.

c. Adjustment procedure

With this background, the following adjustment procedure was designed. First, ECMWF fields (temperature *T,* water vapor mixing ratio *q,* wind components *u* and *v*) were sampled at 33 equally spaced points around the center of the topographic feature (7°N, 80.75°E) east of Colombo at a radius of 2.5° (see Figs. 2, 3). Other sampling radii were tested with results to be discussed later. This sampling radius of 2.5° represents a compromise between a scale large enough to avoid a majority of island effects around Sri Lanka, yet small enough to represent the local large-scale fields at Colombo while eluding most of the topographic flow effects around southern India. Next, multiquadric interpolation (Nuss and Titley 1994) was used with these sampled points to interpolate OA fields to the Colombo location. This interpolation was done at all eight model levels between the surface and 700 hPa. These fields were then vertically interpolated in log pressure to correspond to the sounding pressure levels. Finally, at each sounding

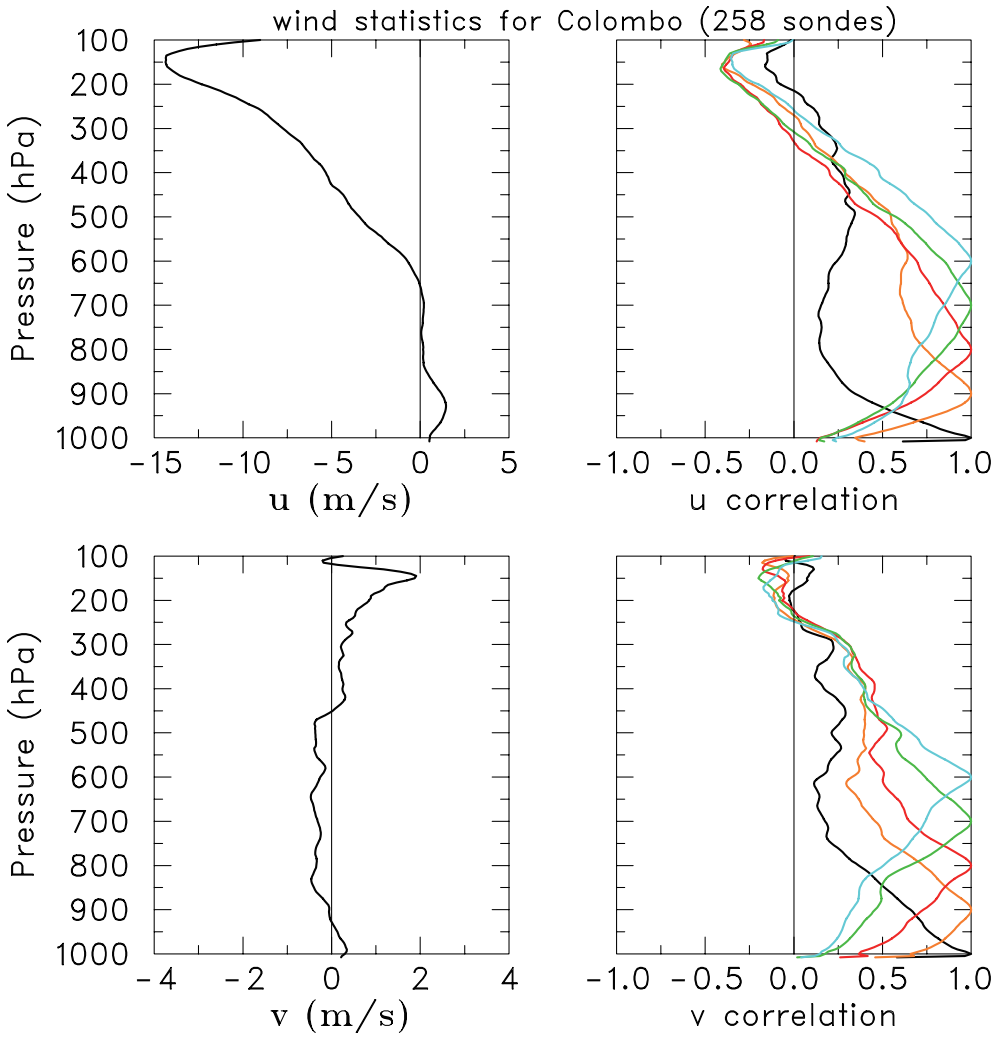

Fig. 7. (Left) mean wind profile at Colombo using unadjusted winds and (right) vertical-lag autocorrelation of wind with base points at 1000, 900, 800, 700, 600 hPa: (top panels) for zonal wind component, (bottom panels) for meridional wind component.

pressure level, model-interpolated fields were merged with actual sounding fields from Colombo to create a blended sounding. The blending is shown here for an arbitrary field f.

$$\begin{aligned} &\cdot \ for: \ p \geq p_{bot}, && f_a = f_i \\ &\cdot \ for: \ p_{bot} > p > p_{top}, && f_a = \frac{[f_i(p - p_{top}) + f_s(p_{bot} - p)]}{(p_{bot} - p_{top})} \\ &\cdot \ for: \ p \leq p_{top}, && f_a = f_s \end{aligned} \quad (1)$$

where f_a is the adjusted field, f_i is the model interpolated field, f_s is the original sounding field, p_{bot} = 900 hPa, and p_{top} = 700 hPa. The rationale behind this simple weighting scheme is as follows. Sounding fields are strongly affected by diurnal and blocking effects below 900 hPa (see Figs. 5, 7). Hence, below this level, adjusted fields are entirely represented with model-interpolated fields. Above 700 hPa, there is little evidence for these effects; therefore, no changes are made to the sounding fields. Between these two levels (i.e., 900 and 700 hPa) the adjusted fields represent a linear transition from model-interpolated fields at 900 hPa to sounding-only fields at 700 hPa. Geopotential height is recomputed for the entire profile using adjusted thermodynamic fields via the hypsometric equation. The procedure defined in (1) was applied

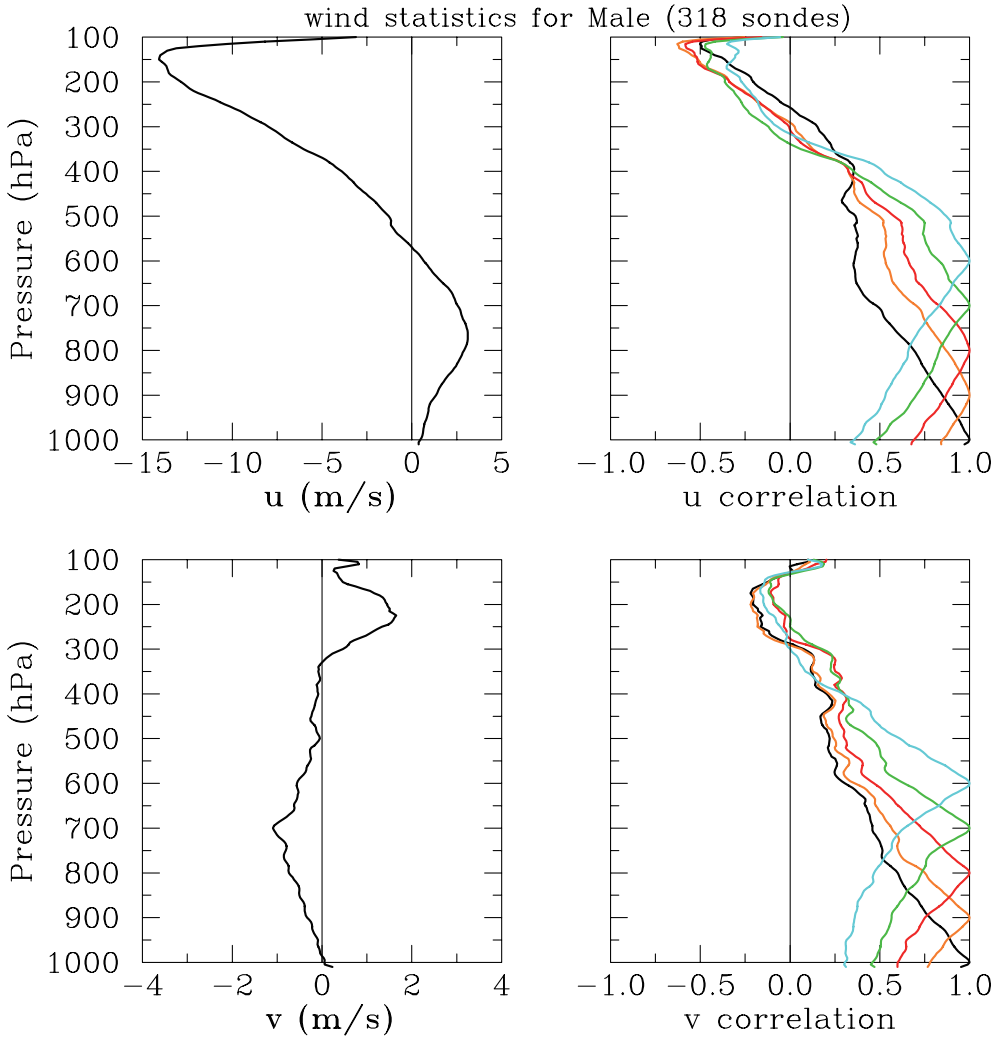

Fig. 8. As in Fig. 7, except using Malé winds.

to all 258 Level 4 (5-hPa resolution) soundings from Colombo[2].

3. Temporal and vertical structure of adjustment

Figure 9 shows the vertical profiles of the mean diurnal cycle at Colombo using the adjusted sounding fields. The adjustment procedure has effectively muted the island's diurnal cycle at low levels making it more representative of open-ocean conditions (e.g., see Malé analysis in Fig. 6) with little distinction between the boundary layer and the free troposphere diurnal variability. The larger diurnal signals in the temperature and zonal-wind fields above 400 hPa are likely related to latent heating and radiative effects due to island-induced convection. Because they are considerably smaller in magnitude than the low-level island effects, no effort was made to adjust these upper-level fields.

The muting of the diurnal cycle is also seen in Fig. 10 by noting the damped high-frequency signal in the time series of adjusted low-level Colombo winds (red curves in first and third panels). Further inspection of these time series shows that, in general, when the low-level flow is westerly, as in the first half of October, then the adjustment acts to increase the low-level westerly flow (second panel). On the other hand, when the low-level flow is easterly, as

[2]Definition of the various sounding data levels can be found in Ciesielski et al . (2014).

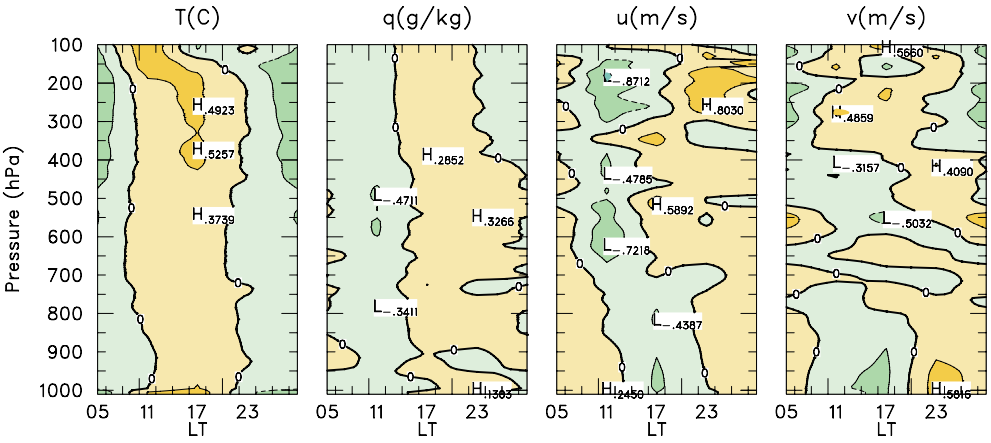

Fig. 9. Diurnal cycle anomaly as in Fig. 5, except for adjusted fields at Colombo.

in mid-November, then the adjustment results in an increase in the low-level easterly flow. This general result is better quantified in Fig. 11 (left panel), which shows the mean adjustment for times when the 850 hPa sounding winds at Colombo were westerly (top panel) and easterly (bottom panel). In the zonal component, the adjustment tends to peak near the surface with mean magnitudes of 2–3 m s^{-1}. Adjustments are slightly larger and extend over a deeper layer when low-level easterlies are present. As one would expect based on the procedure, there is little adjustment in the zonal winds above 850 hPa.

The time series for the low-level meridional flow and its adjustment are shown in the bottom two panel of Fig. 10. In general, the meridional adjustment is small and negative (increased northerlies or decreased southerlies) under most flow conditions. The vertical profiles of the mean meridional adjustments (right panels in Fig. 11) are predominately negative and less than 1 m s^{-1}. While the meridional adjustments are smaller than their zonal counterparts, their vertical extent is somewhat deeper.

The mean adjustments for different sampling radii for the ECMWF fields are also shown in Fig. 11. With smaller sampling radii, the procedure resolves more structure associated with the topographically perturbed flow. As the sampling radii increase, adjustments appear to converge to a single solution that captures the large-scale unperturbed flow. Considerably beyond a 2.5° sampling radius, the procedure begins to sample local flows associated with topographic features in southern India (see Figs. 2, 3). As will be shown later, the 2.5° sampling radius produced the best budget results.

Similar analyses, showing the mean adjustments to temperature (T_a) and water vapor mixing ratio (q_a) as a function of 850 hPa zonal wind direction, are shown in Fig. 12. In both wind regimes, the adjustment results in low-level cooling and drying, which principally reflects the ECMWF low-level cool and dry biases depicted in Fig. 4. The low-level cooling adjustment is more pronounced in the easterly wind regime, suggesting that a downslope warming signal may be present in the Colombo soundings under these flow conditions. Likewise, the smaller dry adjustment near 950 hPa in the easterly wind regime suggests that a downslope drying signal is present near this level in the original soundings.

Further validation of the adjustment procedure is presented in Fig. 13, which shows the vertical-lag autocorrelation of adjusted winds at Colombo. Using adjusted winds, the overall correlation decay rate at low levels more closely resembles that observed at Malé (Fig. 8) with e-folding decay scales greater than 500 hPa. On the other hand, the vertical coupling of the low-level adjusted winds (particularly the zonal component) is too large compared with Malé (i.e., the correlation decay rate is too small). This strong vertical coupling may partially be understood by noting that the adjusted winds are not representative of a point observation but rather of an average over a circle with a 2.5° radius, which tends to reduce vertical shears. Another reason may be related to the vertical coupling inherent in the model winds. To illustrate this point, Fig. 14 shows the vertical-lag autocorrelation of ECMWF winds at the Malé location, which compared with the observed winds (Fig. 8), has a smaller vertical decay rate. While the

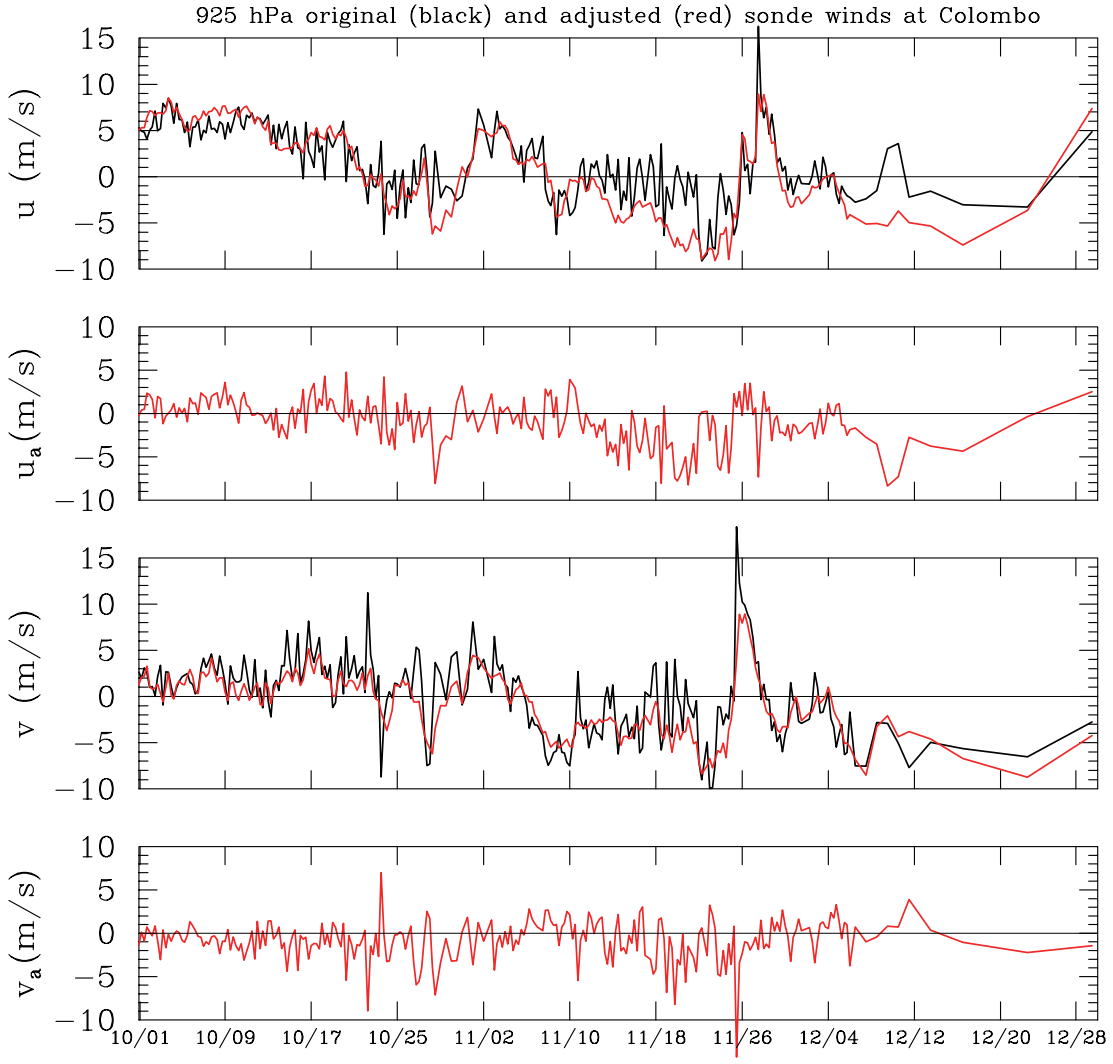

Fig. 10. Time series of the adjustment's impact on the Colombo 925 hPa wind components: (top panel) original (black) and adjusted (red) zonal wind component, (second panel) zonal wind adjustment (adjusted – original), (third panel) original (black) and adjusted (red) meridional wind component, (bottom panel) meridional wind adjustment (adjusted - original).

reasons for this behavior are unclear, the stronger vertical coupling in the model winds compared with the soundings may suggest that vertical diffusion and/or mixing of horizontal momentum in the model is too strong.

4. Impact of adjusted soundings on atmospheric budget analyses

For the analyses presented in this section, gridded fields of horizontal wind components u and v, temperature T, water vapor mixing ratio q, and geopotential height z have been computed at 1° horizontal resolution covering the area from 35°E to 155°E, from 20°S to 20°N, and at 25 hPa vertical resolution using reciprocal multiquadric interpolation (MI) of sounding data (Nuss and Titley 1994, Franke 1982). Given a set of observations of some field H at N distinct locations (x_i, y_i), the multiquadric interpolation equation is

$$H(x, y) = \sum_{i=1}^{N} \alpha_i Q_i(x, y) \qquad (2)$$

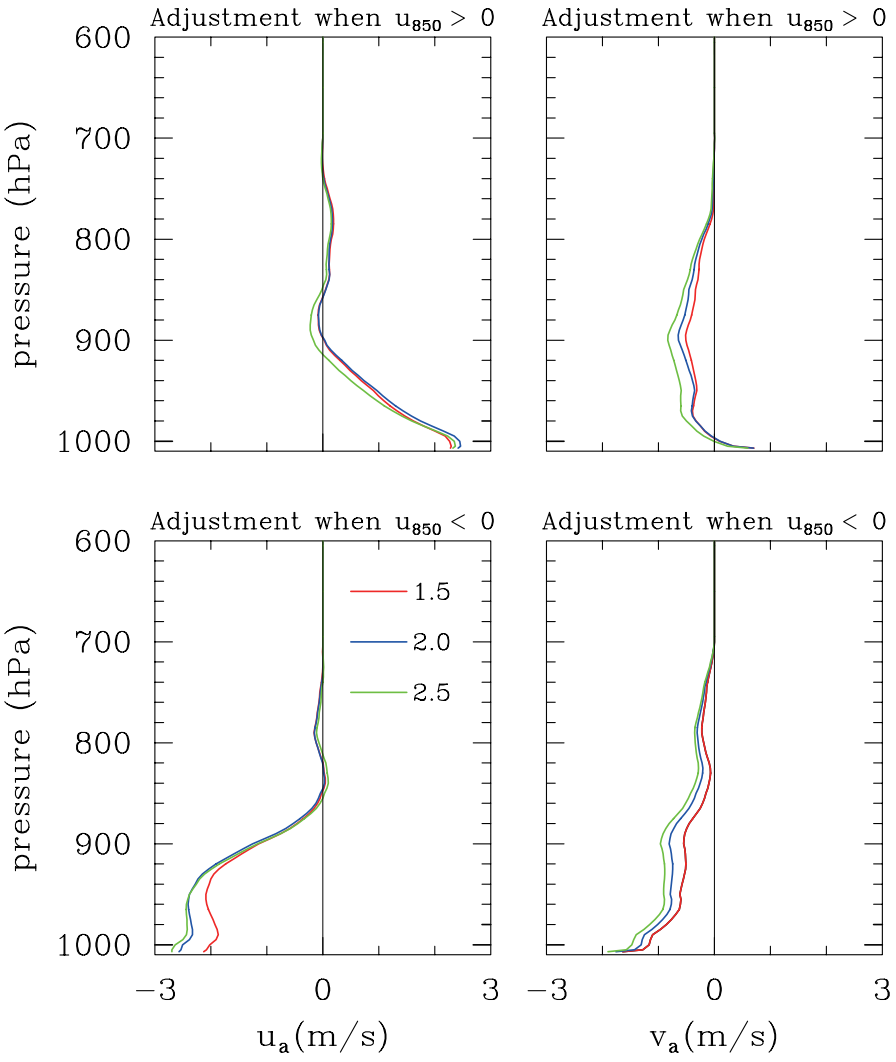

Fig. 11. Sensitivity of adjustment to different sampling radii: (top panels) vertical profile of mean zonal wind adjustment (left) and mean meridional wind adjustment (right) for cases where original 850 hPa zonal wind is westerly, (bottom panels) vertical profile of mean zonal wind adjustment (left) and mean meridional wind adjustment (right) for cases where original 850 hPa zonal wind is easterly.

where the radial basis functions Q_i are given by

$$Q_i(x, y) = \left[(x - x_i)^2 + (y - y_i)^2 + R^2\right]^{-1/2} \qquad (3)$$

for the reciprocal multiquadric method, with $R > 0$ being the tension parameter. The required coefficients α_i are obtained by solving the $N \times N$ linear system that results from inserting the N observations into the following modified version of (2)

$$H(x_j, y_j) = \sum_{i=1}^{N} \alpha_i \left[Q_i(x_j, y_j) + \left(N\lambda\sigma_i^2\delta_{ij}\right)\right] \qquad (4)$$

where λ is a smoothing parameter, σ_i^2 is the mean-squared observation error for the i^{th} observation, and δ_{ij} is the Kronecker delta.

The MI scheme used in (2)–(4) has $N+2$ free parameters (R, λ, σ_i), which must be specified and which determine the characteristics of the interpolation. The tension or multiquadric parameter (R) determines the curvature and width of the interpolating basis functions. The smoothing parameter (λ) sets the amount of spectral low-pass filtering, such that increasing its value produces analyses with fewer small-scale features. Through experimentation, the

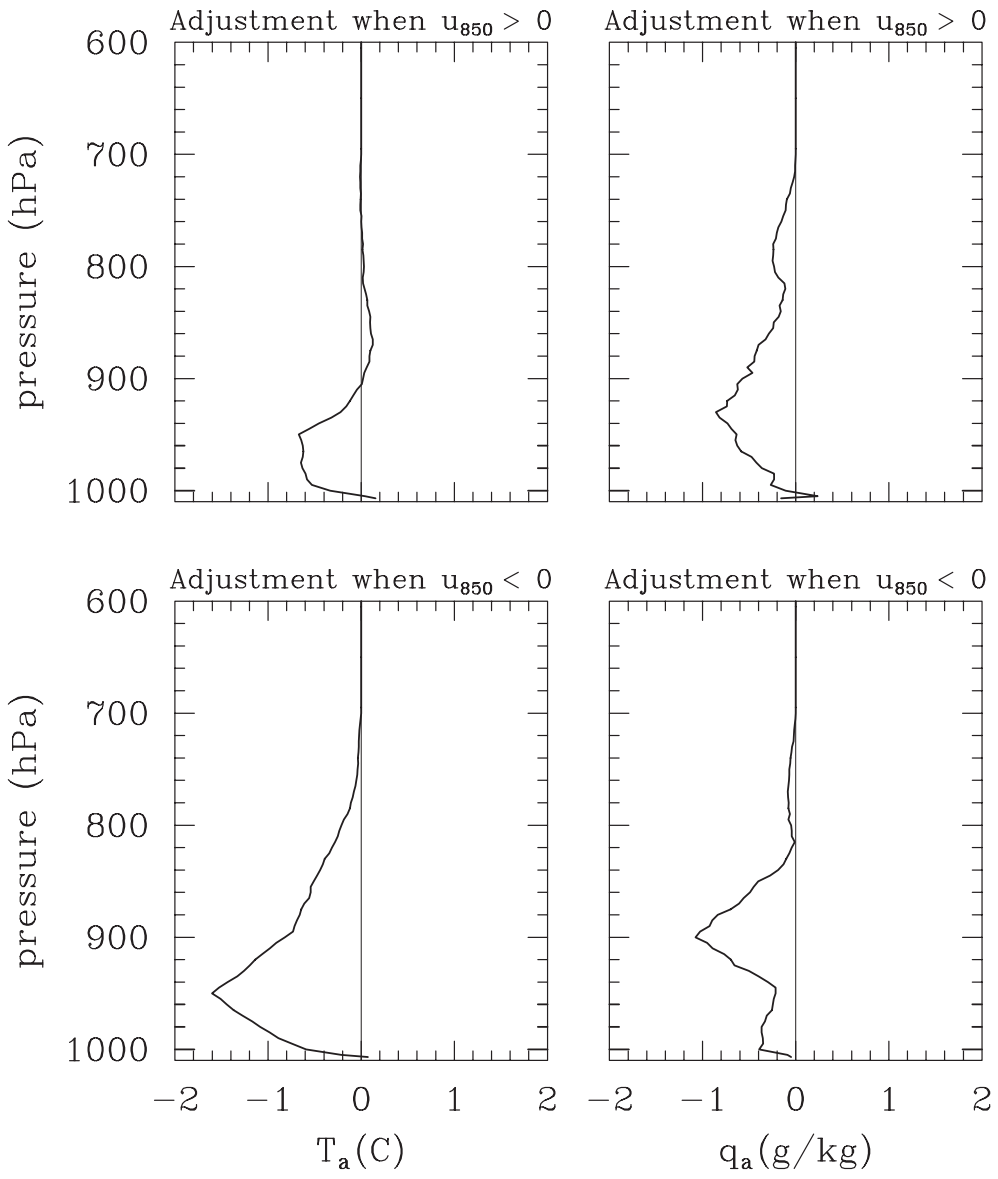

Fig. 12. As in Fig. 11, except for temperature adjustment (left panels) and water vapor mixing ratio adjustment (right panels) computed with sampling radius of 2.5°.

values of $R = 3.5$ and $\lambda = 0.0005$ were chosen for this analysis. While this choice of values may not be best for a given data distribution, it resulted in an optimal balance of consistently accurate (small rms differences between actual sounding data and analyses) and reasonable-looking smooth fields. The σ_i parameters account for observational uncertainty and are specified based on the accuracy of the data type. The values of σ_i chosen for this study include: 1 m s^{-1} for winds, 0.5°C for temperature, 1 g kg^{-1} for water vapor mixing ratio, and 5 m for geopotential height. In constructing the gridded analyses, the Level 4 (5 hPa vertical resolution with quality-control flags) sounding data from the enhanced sounding network (Fig. 1) as well as the larger DYNAMO network (Ciesielski et al. 2014) were used.

To examine the influence of the Colombo sounding data on other locations, multiquadric weighting functions were constructed using MI with a value of one at Colombo's location and zero at other sounding

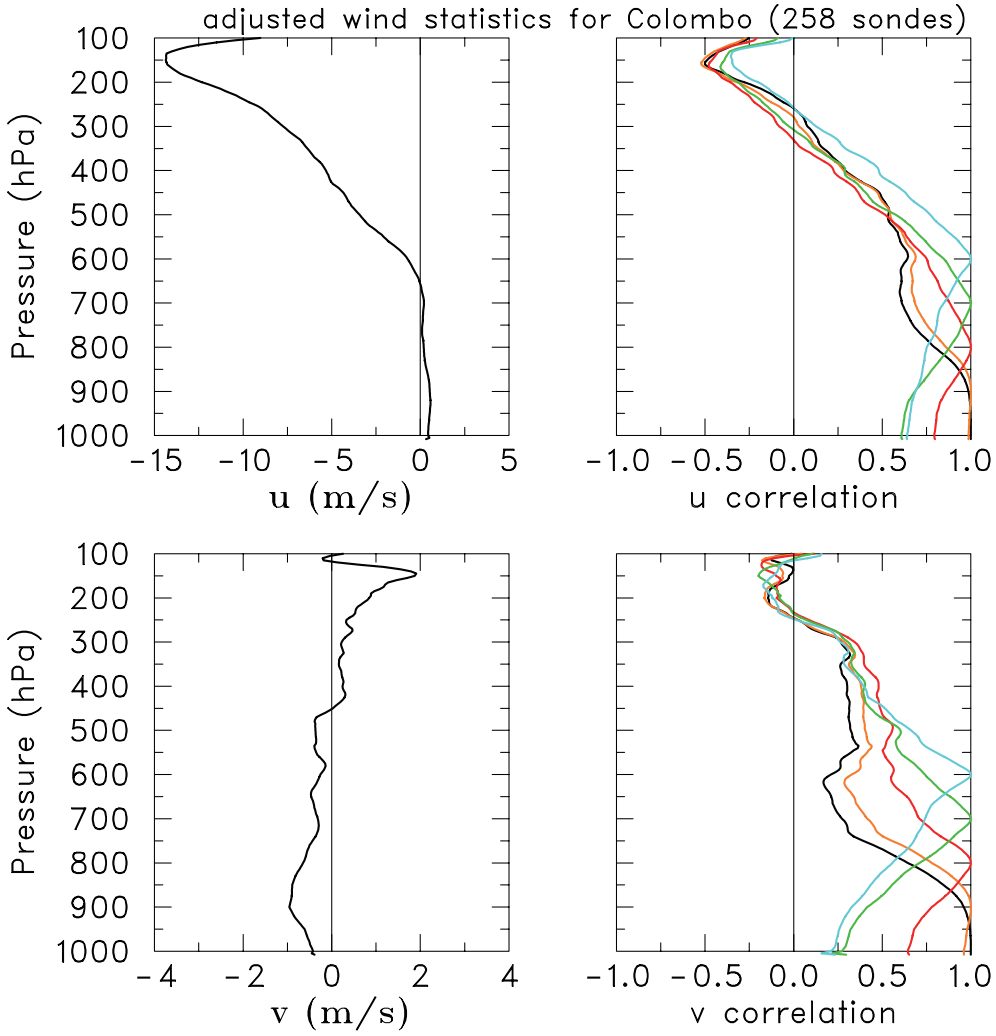

Fig. 13. As in Fig. 7, except using adjusted winds at Colombo.

sites. Using the MI parameters described above, Fig. 15 shows two such multiquadric weighting functions. These weighting functions illustrate how the influence of data at Colombo spreads horizontally with and without the presence of sounding data from sites in India[3]. These functions quantify the degree to which local effects at Colombo are aliased onto the large-scale analyses. Note that Colombo data have minimal influence on analyses south of the equator. Of course, this situation changes somewhat when the *RV* Revelle was not onsite (Eq., 80.5°E) during its port calls.

[3] During DYNAMO sounding data from sites over southern India were available only at 00Z and moreover on less than half of the days.

To illustrate how the Sri Lanka island effects at Colombo can impact atmospheric budgets derived from these gridded analyses, gridded fields were computed using both the original and adjusted Colombo soundings. An example of how the adjustment impacts the gridded fields at a specific time (18Z on 19 November 2011) is shown in Fig. 16. This figure shows the gridded analyses of 925 hPa winds and divergence computed with original (top panel) and (bottom panel) adjusted Colombo winds. Figure 17 shows the vertical profiles of the original and adjusted winds that were used at Colombo for this case. Note that the adjustment at 925 hPa results in a low-level wind shift from weak southerly to strong northeasterly. The gridded analyses reflect this change

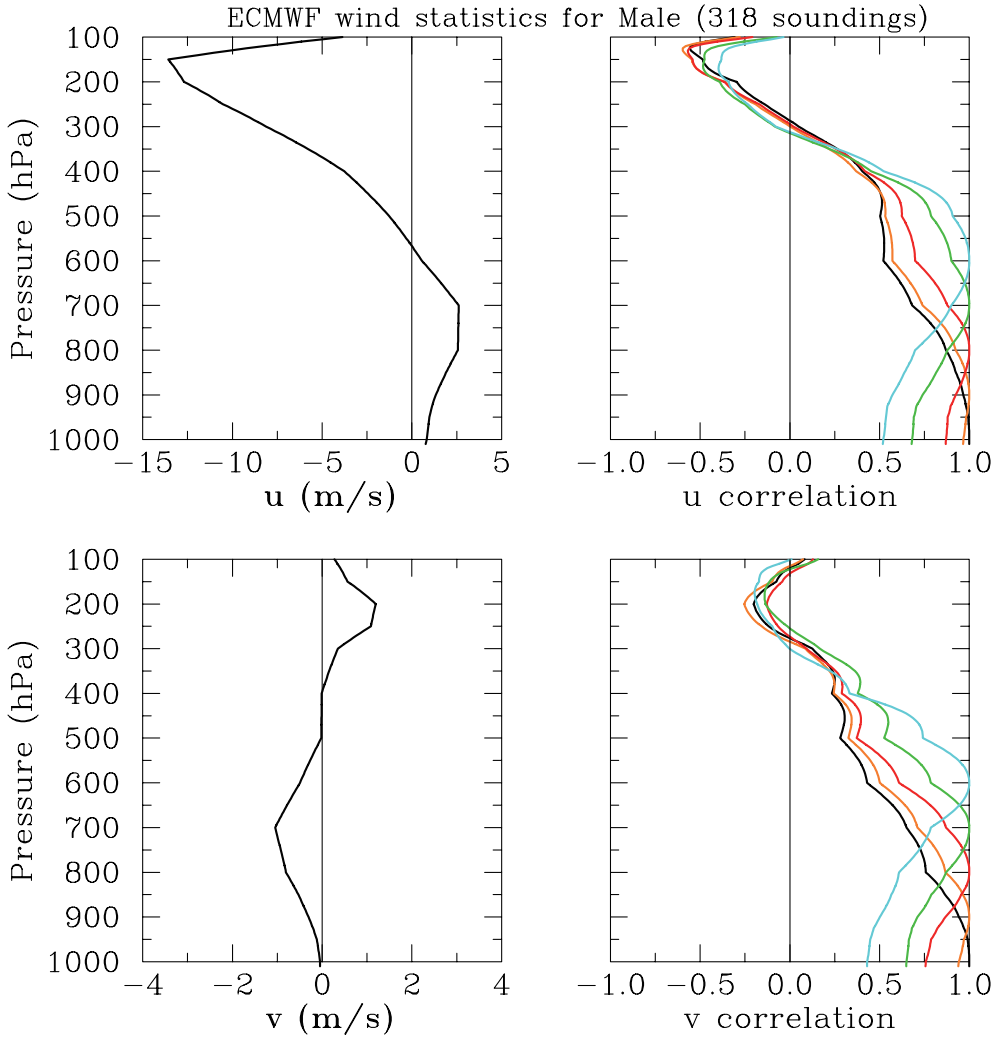

Fig. 14. As in Fig. 8, except using ECMWF OA winds at Malé.

with the divergence field transforming from strongly divergent over the NSA with unadjusted winds to a pattern with strong convergence over the entire NSA with adjusted winds. This case clearly demonstrates how the local blocking effect at Colombo gets aliased onto the larger scale analyses, strongly impacting derived fields.

The impact of the adjusted Colombo soundings on several derived fields averaged over the NSA is shown in Fig. 18. The top two panels show the time series of original and adjusted low-level zonal winds at Colombo and their difference. The modulation of the low-level wind field by the two MJO events during this period is clearly evident in these time series. The zonal-wind adjustment (second panel) shows the general trend of a positive (westerly) adjustment in low-level westerly regimes and a negative (easterly) adjustment in low-level easterly regimes. The impacts on the derived fields (low-level divergence, mid-level vertical motion, and budget-derived rainfall) are shown in the bottom three panels. Here budget-derived rainfall is computed as a residual from the moisture (Q_2) budget and surface evaporation from the WHOI product. In general, the adjustment results in more low-level divergence (convergence), more mid-level subsidence (rising motion), and reduced (increased) rainfall during the westerly (easterly) wind regimes over the NSA. As expected, there was little impact of the adjustment on fields over the DYNAMO southern sounding array (not shown).

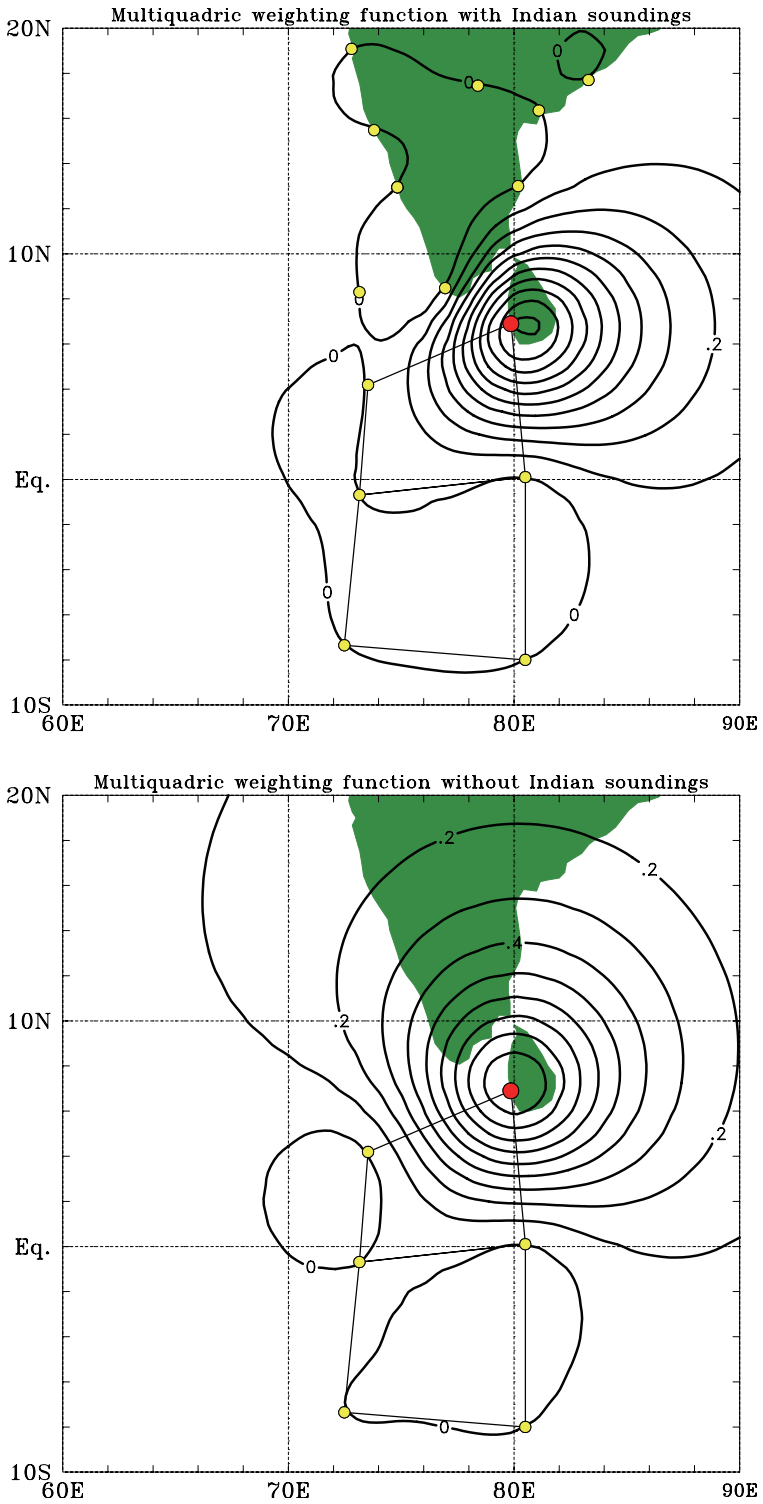

Fig. 15. Multiquadric weighting functions (with contour interval 0.1) illustrating how the influence of data at Colombo spreads horizontally (top) with the presence of Indian soundings and (bottom) without Indian soundings. Weighting functions were constructed by using MI with value at Colombo (red dot) set to one and other sounding locations (yellow dots) set to zero. Northern and Southern Sounding Arrays are indicated with polygons.

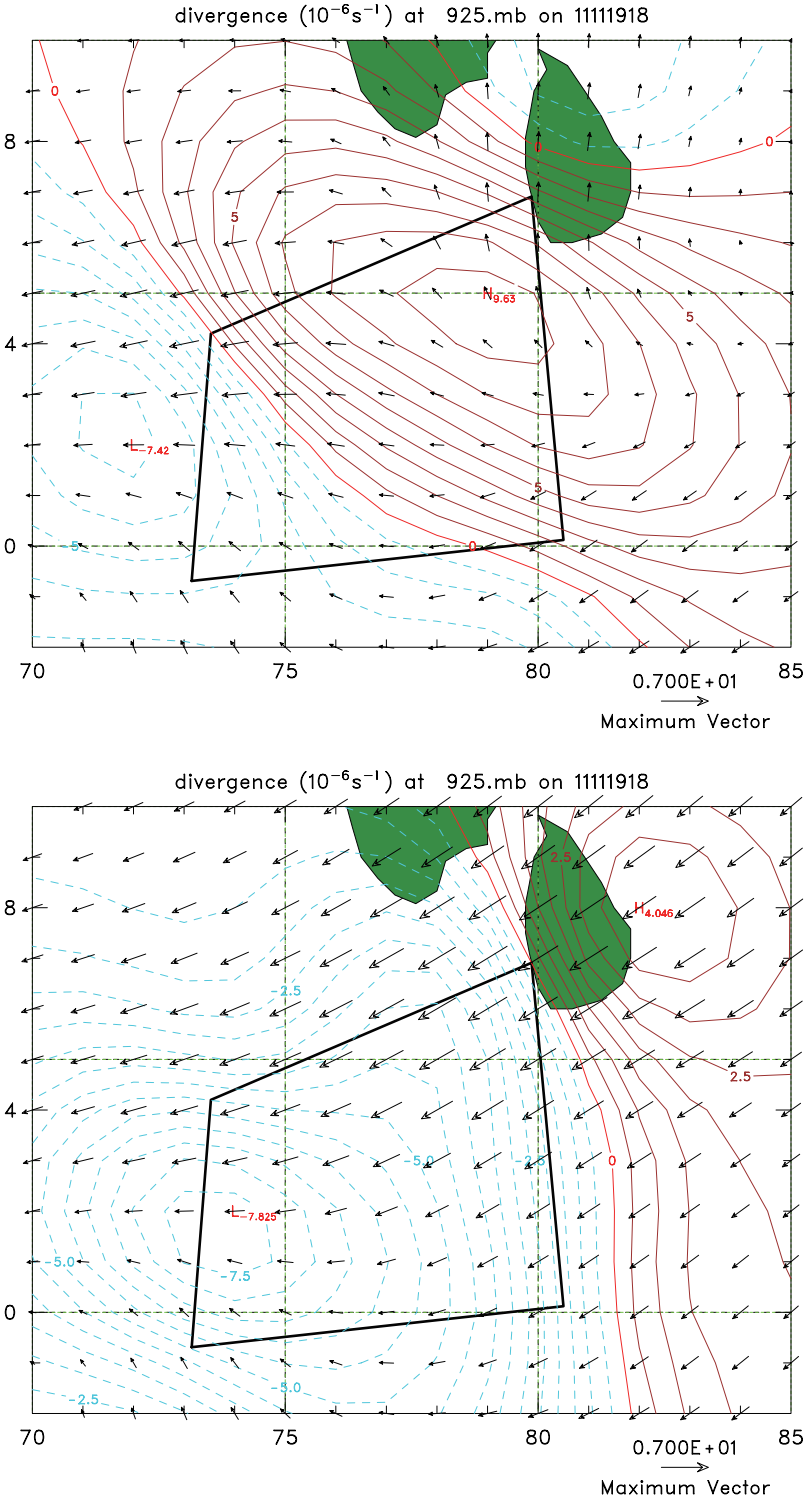

Fig. 16. Gridded analysis of 925 hPa winds and divergence for 18UTC on 19 November 2011: (top panel) based on original fields at Colombo, (bottom panel) based on adjusted fields at Colombo. Scale for wind vectors (m s^{-1}) is shown in lower-right portion of plots. Contour increment for divergence is 0.5×10^{-6} s^{-1}. Blue dashed contours represent convergence and red solid contours divergence. Black quadrilateral shows outline of NSA.

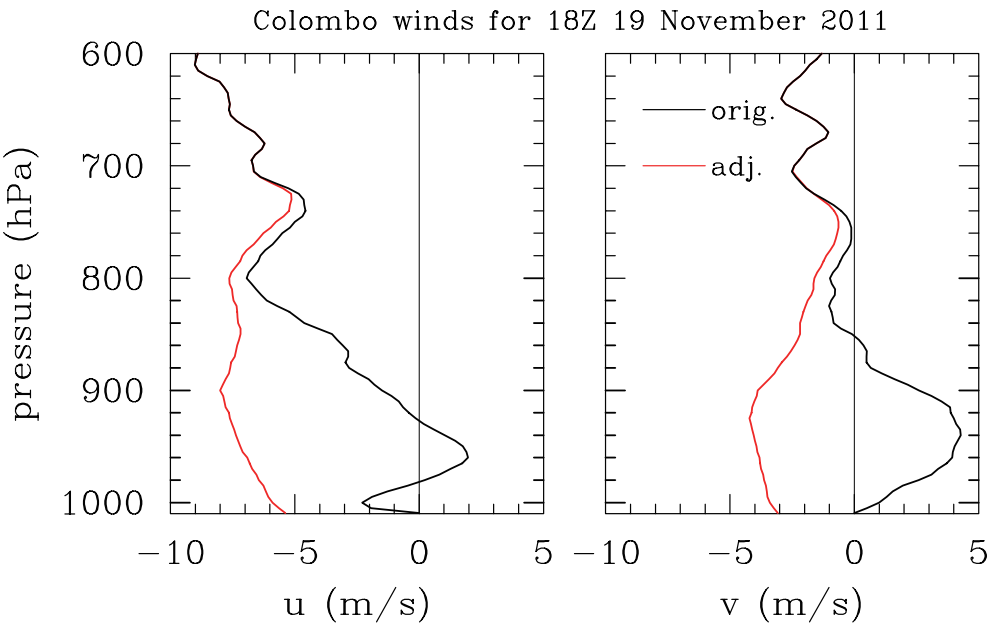

Fig. 17. Vertical profiles of original (black) and adjusted (red) zonal and meridional winds at Colombo for 18UTC on 19 November 2011.

To evaluate whether the adjustment in fact produced desirable changes in the derived fields, Fig. 19 shows the time series of NSA-averaged rainfall estimated from the TRMM 3B42v7 product (Huffman et al. 2007) and that derived from the moisture budget using original and adjusted soundings. The budget-derived rainfall time series computed with original soundings shows periods of unrealistic negative rainfall both in early October and mid-November. Using the adjusted soundings, the periods of negative rainfall, though still present in the former period, have been eliminated in November. Table 1 shows the time-mean of the NSA rainfall estimates computed from the Q_2 budgets using different sampling radii and their correlation to the TRMM rainfall estimates. Note the TRMM mean rainfall over the NSA for this period is 8.9 mm day^{-1}. In comparison with the independent TRMM rainfall estimate, both the mean rainfall and its temporal correlation are improved using adjusted soundings. In addition, the adjusted soundings computed with the largest sampling radius provide the best comparison with the TRMM rainfall estimates both in terms of the mean and transient behavior.

A key aspect in understanding the MJO is the development of convection during its various stages. Typically, the early stages of the MJO development are characterized by shallow convection, which tends to moisten the low- to mid-troposphere over a period of a few weeks. This is followed by progressively deeper convection leading up to the active phase of the MJO (Kikuchi and Takayabu 2004, Mapes et al. 2006, Del Genio et al. 2012, Johnson and Ciesielski 2013). Figure 20 shows the Q_2 field over the NSA computed with both original and adjusted Colombo soundings with the bottom panel giving their difference. In both versions of the analyses, drying, starting mid-month for the October MJO, becomes gradually deeper toward the end of the month, consistent with the notion that the vertical extent of convection gradually shifts from bottom-heavy to top-heavy during the active phase of the MJO (e.g., Kiladis et al. 2005). This sequence is somewhat different in the November MJO event, where in the original analyses, low-level moistening abruptly transitions to deep drying. On the other hand, the Q_2 analyses based on the adjusted soundings shows a more gradual transition into this deep drying stage. The Q_2 difference plot clearly shows this enhanced drying signature caused by the adjusted fields in the early-active phase of the November MJO. Also noteworthy are the changes to vertical moisture advection caused by the adjustment (Fig. 21). Only in the analyses using the adjusted soundings does the vertical moisture advection deepen in a stepwise fashion leading up to the active phase of

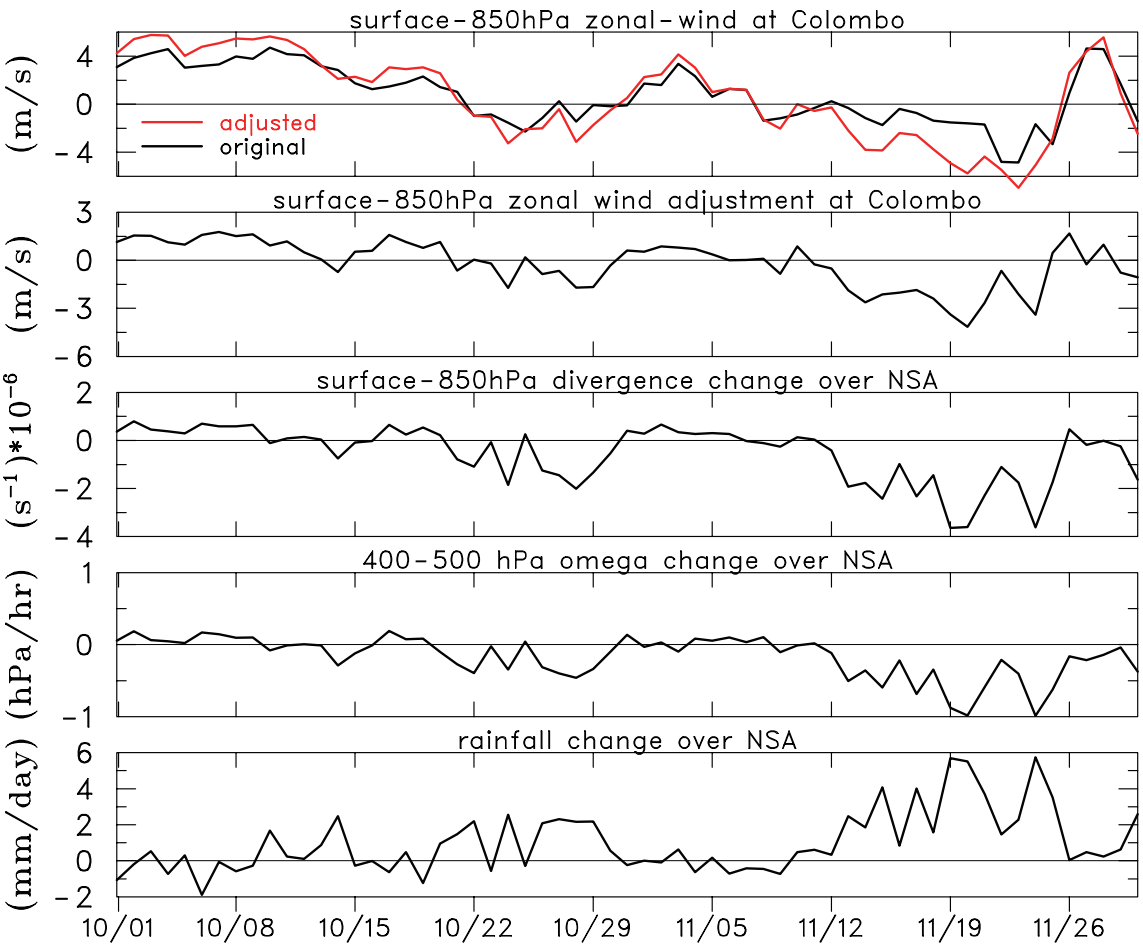

Fig. 18. Time series of the impact of adjusted Colombo winds on various fields and analyses: (top panel) original (black) and adjusted (red) zonal-winds at Colombo averaged at low-levels (surface to 850 hPa layer), (second panel) low-level zonal-wind adjustment (adjusted - original), (third panel) NSA-averaged, low-level divergence change due to wind adjustment, (fourth panel) NSA-averaged mid-level vertical motion change due to wind adjustment, (bottom panel) NSA-averaged Q_2 budget-derived rainfall change due to adjustments.

the November MJO event.

5. Summary

During the DYNAMO field campaign, upper-air soundings launched at the site in Colombo, Sri Lanka, were impacted at low levels by island heating and flow blocking effects caused by elevated terrain to the east of this site. Because of the large spacing between sounding sites over the NSA, these local island effects are aliased onto the larger scale impacting the computation of atmospheric budgets over the sounding array. To mitigate these island effects, a procedure was designed which merges low-level ECMWF operational analysis fields, unperturbed by the island, with observed sounding data.

The impact of the adjustment procedure on Colombo soundings is to effectively mute the island's diurnal cycle at low levels making it more representative of open-ocean conditions. In addition, the procedure results in a mean increase in the low-level westerly winds at Colombo of 2–3 m s^{-1} in westerly flow regimes and a similar increase of the low-level easterly winds in easterly flow regimes. The impact on the meridional winds at Colombo is somewhat smaller with a mean increase in the northerlies of ~1 m s^{-1}. The adjustment also cools (~1°C) and dries (~0.5 g kg^{-1}) the low-levels at Colombo, which partially reflects ECMWF biases over the Indian Ocean, reported previously in Nagarajan and Aiyyer (2004).

In general, over the NSA, the impact of using

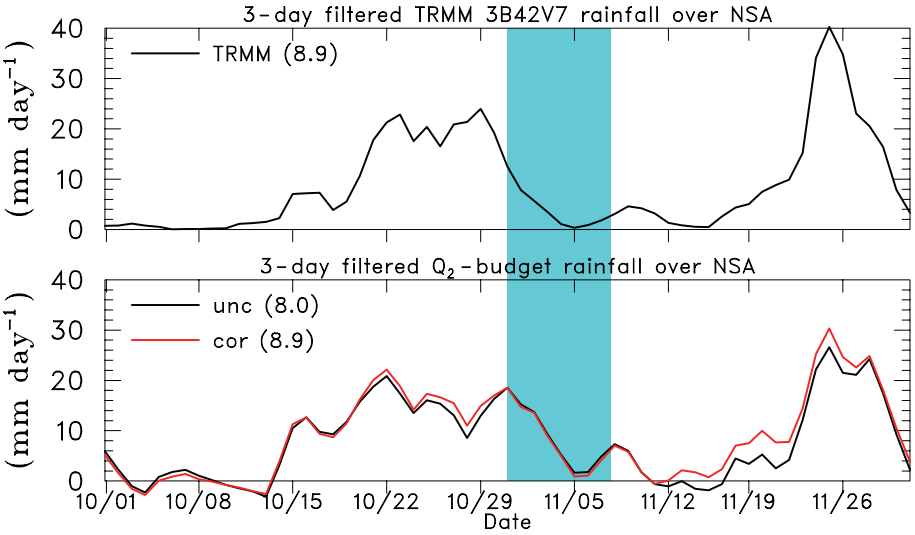

Fig. 19. Time series of 3-day filtered NSA-averaged rainfall: (top panel) from TRMM 3B42 v7 product, (bottom panel) based on Q_2 budget using original (black) and adjusted (red) fields. Blue shading indicates period when *RV* Revelle was off-site and NSA reverts to a triangular shape. Period means are in parentheses.

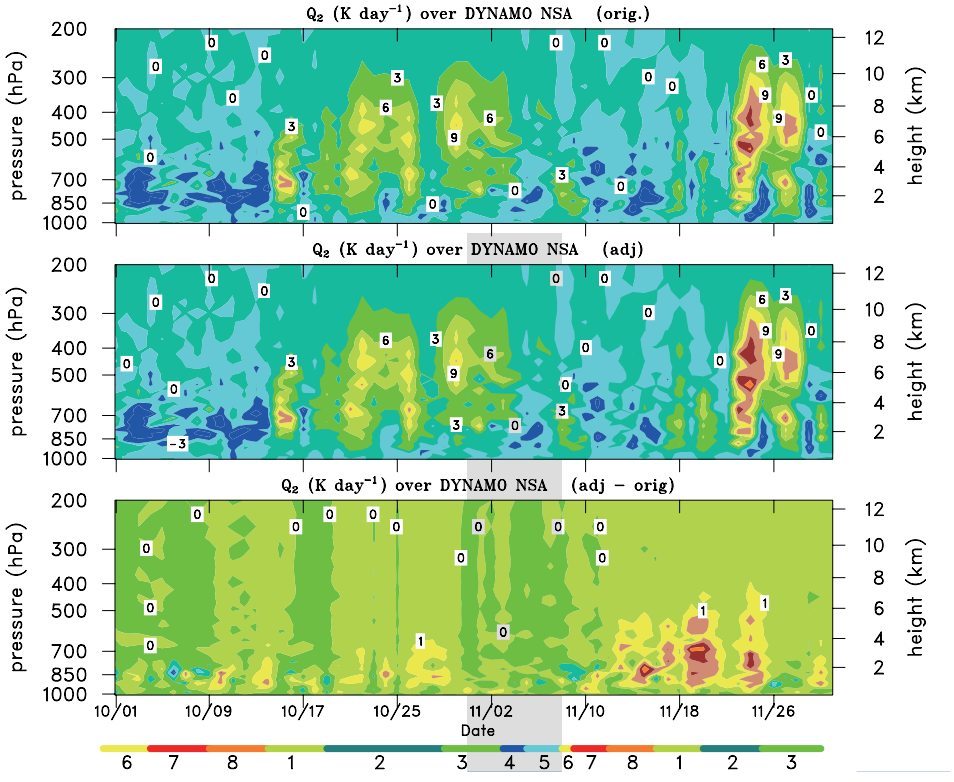

Fig. 20. Time series of Q_2 averaged over NSA: (top panel, contour interval 3 K day^{-1}) computed using original fields, (middle panel, contour interval 3 K day^{-1}) computed using adjusted fields, (bottom panel, contour interval 1 K day^{-1}) difference (adjusted - original). Cool colors imply apparent moistening and warm colors apparent drying. Color bar at bottom indicates MJO index (from Wheeler and Hendon 2004).

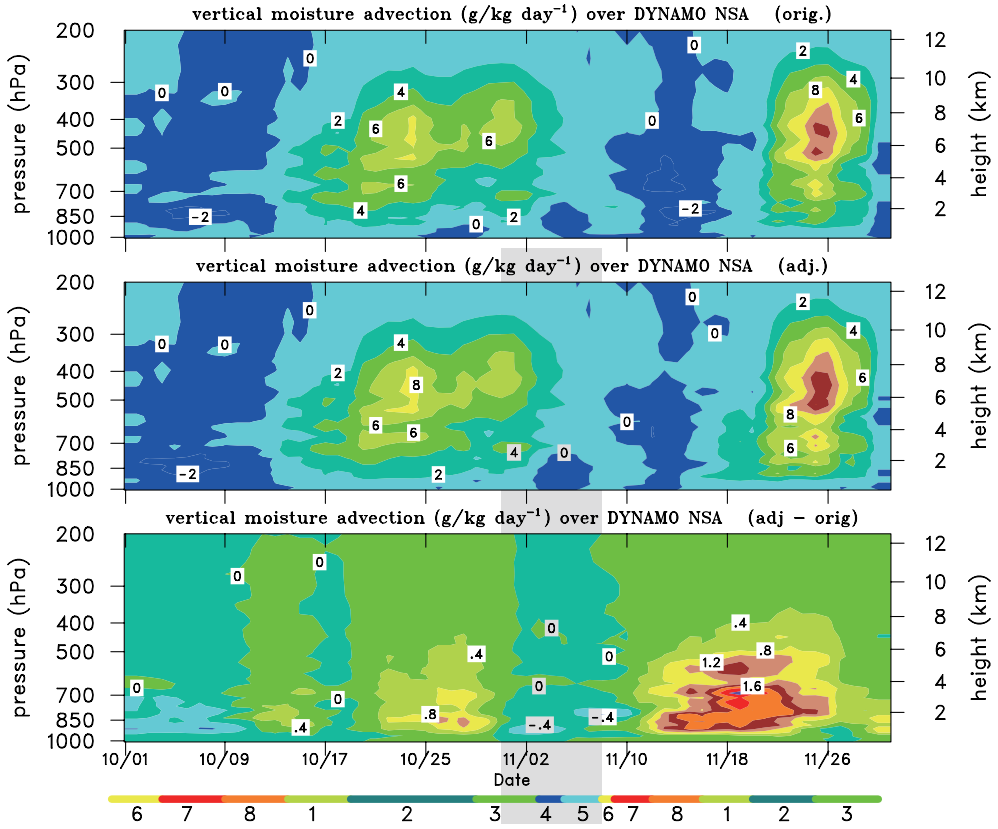

Fig. 21. Same as Fig. 20, except for time series of vertical moisture advection. Here warm colors imply dry advection and cool colors moist advection. Contour intervals: top two panels, 2 K day^{-1}; bottom panel, 0.4 K day^{-1}.

Table 1. NSA-mean rainfall for period 1 October to 30 November 2011 computed from Q_2-budget and its temporal correlation to TRMM 3B42v7 rainfall estimates (first value is correlation based on daily-averaged mean rainfall; number in parentheses is correlation based on 3-day running mean rainfall) for different sampling radii (r).

Rainfall analysis	Mean (mm day^{-1})	Correlation to TRMM rainfall
Original fields	8.0	0.79 (0.86)
Adjusted fields (r = 1.5°)	8.5	0.83 (0.89)
Adjusted fields (r = 2.0°)	8.7	0.84 (0.90)
Adjusted fields (r = 2.5°)	8.9	0.84 (0.91)

the adjusted Colombo soundings results in more low-level divergence (convergence), more mid-level subsidence (rising motion), and reduced (increased) rainfall during the low-level westerly (easterly) wind regimes over the NSA. In comparison with independent TRMM rainfall estimates, both the mean budget-derived rainfall and its temporal correlation are improved using the adjusted soundings. In addition, use of the adjusted fields results in a more realistic moisture budget analysis, particularly during the build-up phase of the November MJO when a more gradual deepening of apparent drying is observed. *In conclusion, use of adjusted soundings at Colombo have effectively mitigated the local island effects*

(diurnal heating and topographic flow blocking) of Sri Lanka, and have produced a beneficial impact on the NSA analyses and budgets, such that they are now better representative of large-scale, open-ocean conditions.

The original as well as adjusted Colombo soundings are available from the EOL DYNAMO data archive: http://data.eol.ucar.edu/master_list/?project=DYNAMO.

Acknowledgments

We thank Chuck Long and Chidong Zhang for their insightful suggestions. We acknowledge ECMWF for providing their operational analysis and Steve Williams of NCAR EOL for providing us with a convenient method for accessing it. This research was supported by NSF grants AGS-1059899 and AGS-1138353 and the National Aeronautics and Space Administration under grant NNX10AG81G.

References

Ciesielski, P. E., Y. Hungjui, R. H. Johnson, K. Yoneyama, M. Katsumata, C. N. Long, J.Wang, S. M. Loehrer, K. Young, S. F. Williams, W. Brown, J. Braun, and T. V. Hove, 2014: Quality-controlled upper-air sounding dataset for DYNAMO/CINDY/AMIE: Development and corrections. *J. Atmos. Oceanic Technol.*, **31**, 741–764.

Del Genio, A. D., Y. Chen, D. Kim, and M.-S. Yao, 2012: The MJO transition from shallow to deep convection in CloudSat/CALIPSO and GISS GCM simulations. *J. Climate*, **25**, 3755–3770.

Franke, R., 1982: Scattered data interpolation: Tests of some methods. *Math. Comput*., **38**, 181–200.

Huffman, G. J., R. F. Adler, D. T. Bolvin, G. Gu, E. J. Nelkin, K. P. Bowman, Y. Hong, E. F. Stocker, and D. B. Wolff, 2007: The TRMM multi-satellite precipitation analysis: Quasi-global, multi-year, combined-sensor precipitation estimates at fine scale. *J. Hydrometeor.*, **8**, 38–55.

Johnson, R. H., and P. E. Ciesielski, 2002: Characteristics of the 1998 summer monsoon onset over the Northern South China Sea. *J. Meteor. Soc. Japan*, **80**, 561–578.

Johnson, R. H., and P. E. Ciesielski, 2013: Structure and properties of Madden-Julian Oscillations deduced from DYNAMO sounding arrays. *J. Atmos. Sci.*, **70**, 3157–3179.

Katsumata, M., P. E. Ciesielski, and R. H. Johnson, 2011: Evaluation of budget analyses during MISMO. *J. Appl. Meteor. Climatol.*, **40**, 241–254.

Kiladis, G. N., K. H. Straub, and P. T. Haertel, 2005: Zonal and vertical structure of the Madden–Julian Oscillation. *J. Atmos. Sci.*, **62**, 2790–2809.

Kikuchi, K., and Y. N. Takayabu, 2004: The development of organized convection associated with the MJO during TOGA COARE IOP: Trimodal characteristics. *Geophys. Res. Lett*., **31**, L10101, doi:10.1029/2004GL019601.

Mapes, B. E., S. Tulich, J. Lin, and P. Zuidema, 2006: The mesocale convection life cycle: Building block or prototype for large-scale tropical waves? *Dyn. Atmos. Oceans*, **42**, 3–29.

Nagarajan, B., and A. Aiyyer, 2004: Performance of the ECMWF operational analyses over the tropical Indian Ocean. *Mon. Wea. Rev.*, **132**, 2275–2282.

Nuss, W. A., and D. W. Titley, 1994: Use of multiquadric interpolation for meteorological objective analysis. *Mon. Wea. Rev.*, **122**, 1611–1631.

Wheeler, M. C., and H. H. Hendon, 2004: An all-season real-time multivariate MJO index: Development of an index for monitoring and prediction. *Mon. Wea. Rev.*, **132**, 1917–1932.

Yanai, M., S. Esbensen, and J.-H. Chu, 1973: Determination of bulk properties of tropical cloud clusters from large-scale heat and moisture budgets. *J. Atmos. Sci.*, **30**, 611–627.

Yoneyama, K., M. Katsumata, K. Mizuno, M. Yoshizaki, R. Shirooka, K. Yasunaga, H. Yamada, N. Sato, T. Ushiyama, Q. Moteki, A. Seiki, M. Fujita, K. Ando, H. Hase, I. Ueki, T. Horii, Y. Masumoto, Y. Kuroda, Y. N. Takayabu, A. Shareef, Y. Fujiyoshi, M. J. McPhaden, V. S. N. Murty, C. Yokoyama, and T. Miyakawa, 2008: MISMO field experiment in the equatorial Indian Ocean. *Bull. Amer. Meteor. Soc*., **89**, 1889–1903.

Yoneyama, K., C. Zhang, and C. N. Long, 2013: Tracking pulses of the Madden–Julian Oscillation. *Bull. Amer. Meteor. Soc.*, **94**, 1871–1891.

Yu, L., and R. A. Weller, 2007: Objectively analyzed air–sea heat fluxes for the global ice-free oceans (1981–2005). *Bull. Amer. Meteor. Soc*., **88**, 527–539.

Zubair, L., 2002: Diurnal and seasonal variation in surface wind at Sita Eliya, Sri Lanka. *Theor. Appl. Climatol*., **71**, 119–127.